Analytica Chimica Acta 1221 (2022) 340118

Contents lists available at ScienceDirect

Analytica Chimica Acta

journal homepage: www.elsevier.com/locate/aca

Smartphone-based magneto-immunosensor on carbon black modified screen-printed electrodes for point-of-need detection of aflatoxin B1 in cereals

Safiye Jafari [a,b], Loïc Burr [b], Davide Migliorelli [b], Roger Galve [c], M.-Pilar Marco [c], Katrina Campbell [d], Chris Elliott [d], Michele Suman [e], Shana J. Sturla [a], Silvia Generelli [b,*]

[a] Department of Health Sciences and Technology, ETH Zürich, Schmelzbergstrasse 9, 8092, Zürich, Switzerland
[b] CSEM SA, Centre Landquart, Bahnhofstrasse 1, 7302, Landquart, Switzerland
[c] Nanobiotechnology for Diagnostics (Nb4D), Institute for Advanced Chemistry of Catalonia (IQAC) of the Spanish Council for Scientific Research (CSIC), Jordi Girona 18-26, 08034, Barcelona, Spain
[d] Institute for Global Food Security, School of Biological Sciences, Queen's University, 19 Chlorine Gardens, Belfast, BT9 5DL, UK
[e] Barilla SpA - Analytical Food Science /Food Safety&Authenticity Research Manager, Parma, Italy

HIGHLIGHTS

- Smartphone-based electrochemical detection of aflatoxin B1 in cereals was achieved.
- The electrode was modified with carbon black nanomaterial.
- Validation confirmed a detection capability of 2 μg/kg, the EU MRL for aflatoxin B1.
- AflaESense app was developed to visualize the result in a traffic-light type format.

GRAPHICAL ABSTRACT

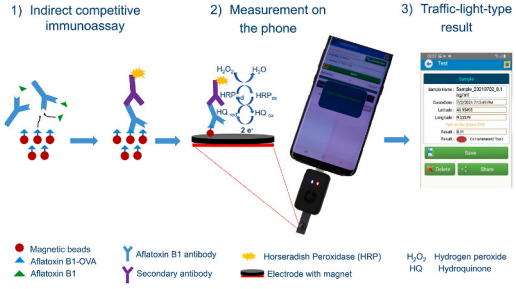

ARTICLE INFO

Keywords:
Smartphone-based immunosensor
Carbon black
Electrochemical biosensor
Point-of-need detection
Aflatoxin B1
Validation

ABSTRACT

Considering the complexities and speed of modern food chains, there is an increasing demand for point-of-need detection of food contaminants, particularly highly regulated chemicals and carcinogens such as aflatoxin B1. We report a user-friendly smartphone-based magneto-immunosensor on carbon black modified electrodes for point-of-need detection of aflatoxin B1 in cereals. For buffered analyte solutions and a corn extract sample, the assay demonstrated a low limit of detection of 13 and 24 pg/mL, respectively. The assay was also highly reproducible, exhibiting mean relative standard deviations of 3.7% and 4.0% for the buffered analyte and corn extract samples. The applicability of the assay was validated on the basis of EU guidelines and the detection capability was lower than or equal to 2 μg/kg, which is the EU maximum residue limit for aflatoxin B1 in cereals. False-positive and false-negative rates were less than 5%. Additionally, an open-source android application, AflaESense, was designed to provide a simple interface that displays the result in a traffic-light-type format, thus minimizing user training and time for data analysis. AflaESense was used for smartphone-based screening of spiked corn samples containing aflatoxin B1 (0.1, 2, and 10 ng/mL), and naturally contaminated corn containing 0.15 ng aflatoxin B1/mL. The measured values were in close agreement with spiked concentrations ($r^2 = 0.99$), with recovery

* Corresponding author.
E-mail address: silvia.generelli@csem.ch (S. Generelli).

https://doi.org/10.1016/j.aca.2022.340118
Received 16 February 2022; Received in revised form 20 June 2022; Accepted 22 June 2022
Available online 24 June 2022

values ranging between 80 and 120%. Finally, contaminated samples correctly triggered a red alert while the non-contaminated samples led to the display of a green color of AflaESense. To the best of our knowledge, this is the first smartphone-based electrochemical system effective for screening samples for contamination with aflatoxin B1.

1. Introduction

Aflatoxins are the secondary metabolites of *Aspergillus flavus* and *Aspergillus parasiticus* fungi, which contaminate a wide range of food and feed products including grains, nuts, and milk. They are chemically stable and cannot be eliminated by cooking, boiling, nor other food processing methods [1]. The most potent aflatoxin, aflatoxin B1, is a known human carcinogen (International Agency for Research on Cancer Group 1), and its dietary exposure is associated with the development of liver cancer [2,3]. The EU maximum residue limit (MRL) for aflatoxin B1 in food and feed is 2 μg/kg [4–8]. At the beginning of 2020, in the EU rapid alert system for food safety, there were at least 100 notifications for aflatoxin B1, which were mostly confirmed contamination alerts [9]. Aflatoxin B1 contamination should be managed by strict food safety measures, however, the most effective tests for contamination are laboratory-based methods. Considering this limitation, together with the frequent occurrence of aflatoxin B1 contamination and its large health risk, there is an increasing need for on-site and point-of-need screening of aflatoxin B1 in every step of the food chain from farms to border inspections and even supermarkets [10].

The most common screening method for aflatoxin B1 detection is an enzyme-linked immunosorbent assay (ELISA) assay, based on robust antibody binding to the analyte, providing specific and sensitive detection with a limit of detection (LOD) lower than 2 μg/kg [4]. For precise quantification, such as needed for confirmation of suspected contamination after preliminary screening by ELISA, the most used methods are liquid chromatography combined with fluorescence detection or mass spectrometry [11–14]. These laboratory-based methods require transferring samples to a central laboratory to be tested by experts using expensive equipment and are not point-of-need compatible nor user-friendly for non-experts [10].

In recent years, the development of miniaturized and cost-effective potentiostats with smartphone connectivity has enabled the development of smartphone-based electrochemical biosensors with point-of-need detection compatibility [15,16]. Improved accessibility and user-friendliness of smartphone-based devices in combination with the sensitive and quantitative detection capability of immunosensors make them a promising candidate for point-of-need food analysis [17,18]. For example, integrated exogenous antigen testing (iEAT) is a smartphone-based magneto-immunosensor developed for food protein antigen detection with an LOD of 0.1 mg/kg [19]. The pocket-size potentiostat connected to a smartphone through Bluetooth was used for electrochemical measurements of protein antigens. With this tool, the hazard levels of allergens were displayed with a simple warning label on a customized application on the phone, minimizing the need for user training. Additionally, a smartphone-based lab-on-a-glove was developed for the qualitative detection of organophosphorus compounds on the surface of fruit and vegetables [20]. The glove was coupled with a miniaturized potentiostat capable of real-time wireless data transmission to a smartphone, and data was visualized as a current plot on the smartphone, which required further data analysis by experts. Smartphone-based optical biosensors for detecting aflatoxin B1 using the smartphone camera have been developed previously; they have an LOD of 10–20 ng/mL and suffer from environmental light interferences and smartphone variability [21,22]. The use of an electrochemical sensor may overcome these limitations, however, to the best of our knowledge, there is no reported smartphone-based electrochemical immunosensor for aflatoxin B1.

To improve the sensitivity of electrochemical immunosensing for the detection of aflatoxin B1, several studies have reported different strategies for signal amplification. A competitive immunosensor based on antibody-functionalized mesoporous carbon nanoparticles was developed to detect aflatoxin B1. The detection limit for aflatoxin B1 in the buffer was 3 pg/mL [23]. Additionally, nafion-modified glassy carbon electrodes were used to electrostatically immobilize the aflatoxin B1 antibody on the electrode. The real sample analysis was reported in Ten spiked peanut samples having different levels of aflatoxin B1 ranging from 20 to 1 ng/mL and the results were statistically equivalent to the data generated with a commercial ELISA kit analysis. More recent studies also reported using complex nanomaterials such as gold nanoparticle-tungsten disulfide-multi-walled carbon nanotubes and graphene quantum dots on molybdenum disulfide nanosheets modified indium tin oxide to create electrodes with an LOD values as low as 0.068 pg/mL and 90 pg/mL, respectively [24,25]. Despite the low LOD and high sensitivity of these methods, the complicated synthesis and electrode modification limit the mass production of such electrodes.

To achieve a lower limit of detections, carbon black nanomaterial (CB) has been introduced as an alternative signal amplification strategy to carbon nanotubes, graphene, and gold nanoparticles, since it can provide the same or higher levels of signal amplification at a lower cost (c.a. 1 €/Kg) [26]. Recent studies showed that electrode modification with CB provided a larger electroactive surface area, higher electrical conductivity, and faster charge transfer rates at the electrode surface [27,28]. Furthermore, CB has been used in combination with other nanomaterials and polymers for electrode modification, such as with platinum nanoparticles and poly(lactic acid) [29,30]. While these combinations achieved higher signal amplification and better electroanalytical performance, the use of CB alone can simplify the electrode modification process such that it can be done using commercial automated reagent dispensers, and the stability of the CB suspension leads to high reproducibility in electrode modification. Indeed, CB-based electrochemical sensors have been used to detect diverse analytes including hydrogen peroxide [31], drugs [32], neurotransmitters [33], phenolic compounds [34], molybdenum disulfide in olive oil [35], and pesticides in water [36]. However, to the best of our knowledge, CB has not been used to detect aflatoxin B1. spec.

In this study, we used CB for signal amplification to develop a smartphone-based magneto-immunosensor to detect aflatoxin B1 in cereals. For this purpose, screen-printed electrodes were modified with CB (SPE-CB). We characterized the electrochemical performance of SPE-CB using cyclic voltammetry (CV) and electrochemical impedance spectroscopy (EIS). Then, we evaluated the analytical performance of SPE-CB for the detection of aflatoxin B1 using a magneto-immunosensing strategy based on indirect competitive ELISA. We validated the magneto-immunosensor based on the current EU guideline for investigating biosensor applicability for aflatoxin B1 screening [37]. Finally, we integrated the sensor with a smartphone-based user-friendly open-source android application, which we called AflaESense. The application reported the result in a traffic-light-type format, ideal for use by non-experts. AlfaESense allows a first screening on-field avoiding the cost of standard lab analysis for all the samples. In this way, only the flagged samples (red-light results) will be sent to the lab for confirmatory tests which will have a tremendous impact on lowering the final cost.

2. Material and methods

2.1. Reagents, immunoreagents & equipment

Magnetic beads, Dynabeads™ MyOne™ Tosylactivated (Cat. No 65502) were purchased from Thermo Fisher Scientific (Waltham, Massachusetts, United States). Other chemicals such as aflatoxin B1, aflatoxin B2, aflatoxin G1, aflatoxin G2 solutions, boric acid, sodium borate, ammonium sulfate, bovine serum albumin (BSA), sodium hydroxide, sodium citrate, citric acid, Tween 20, hydrogen peroxide, hydroquinone (HQ), methanol, ethanol, dimethylformamide (DMF), potassium chloride, potassium ferricyanide, potassium ferrocyanide, were purchased from Sigma-Aldrich (St. Louis, Missouri, United States). The anti-mouse IgG (Fab specific)–peroxidase antibody produced in goat (HRP-pAb) (Pro. No 9917) was purchased from Sigma. The monoclonal antibody specific for aflatoxin B1 (AFB1-mAb) was produced according to the procedures outlined in Oplatowska et al., 2016 [38]. The aflatoxin B1−ovalbumin conjugate (AFB1-OVA) was produced with a modification of the method reported by Refs. [39,39]. The certified blank and naturally contaminated grain and corn samples were kindly provided by FoodSmartphone project partners: Prof. Michel Nielen (Wageningen Food Safety Research (WFSR), part of Wageningen University & Research, Wageningen, The Netherlands); Prof Chris Elliott (Institute for Global Food Security, School of Biological Sciences, Queen's University Belfast); Dr. Michele Suman (Barila S.p.A., Advanced Laboratory Research, Barilla Research Labs, Parma, Italy).

All buffer solutions were prepared with MilliQ water from Milli-Q Direct 8, Millipore device. The composition of the phosphate buffer saline (PBS) solution was 0.01 M phosphate buffer in a 0.8% (w/v) NaCl solution, pH 7.5, while in PBST as washing buffer, 0.05% (v/v) Tween 20 was also added. The reagent dilution buffer was PBST with 1% BSA. The coating buffer, 0.1 M sodium borate buffer pH 9.5 was used for the coupling of magnetic beads with AFB1-OVA conjugate. The substrate solution consisted of 1 mM H_2O_2, 1 mM HQ in citrate-phosphate buffer 0.05 M, potassium chloride 0.1 M, pH 5.

Magnetic separation was performed in 2 mL Eppendorf tubes using a MagnaRack (Cat. No. CS15000) purchased from Invitrogen (Carlsbad, California, United States). Screen-printed electrodes (SPE) were printed in-house using a semi-automatic screen-printing machine (DEK 248) on a flexible polyester sheet (Autostat CT, Wantage, UK). The graphite, silver, silver/silver chloride, and dielectric ink were purchased from Gwent (Pontypool, UK). The SPE consisted of circular graphite with a 2 mm diameter as the working electrode, a silver/silver chloride arc as the reference electrode, and a graphite arc as the counter electrode. CB (N220) was obtained from Cabot Corporation (Ravenna, Italy). The ultrasonic homogenizer, Hielscher's UP 200ST from Hielscher GmbH (Teltow, Germany) was used to prepare the CB dispersion with an amplitude of 80%, a pulse of 30%, and energy of 3800 W/mL. The CNC milling machine Bohr-Fräsmaschine BF20 L Vario Article No. 333 8122 used to fabricate the magnetic-holder was from Optimum, Germany. The drilling head was from Stadelmann Maschinen AG, Schötz, Switzerland with cutting tools from favora with a diameter of 1 mm for the top part and 2 mm for the bottom part. Electrochemical measurements were performed using a MultiPalmSens4 potentiostat and MultiTrace4 software purchased from PalmSens (The Netherlands). Smartphone-based measurements were performed on Sensit Smart purchased from PalmSens (The Netherlands). Data analysis was performed using GraphPad Prism 9 software.

2.2. Coupling of magnetic beads with AFB1-OVA conjugate

The AFB1-OVA conjugate, which will function as the competing antigen, was coupled to the tosyl-activated magnetic beads according to the provider's protocol (dynabeads_myone_tosylactivated_man.pdf). First, Dynabeads MyOne tosyl-activated magnetic beads stock solution 100 mg/mL was vortexed for 30 s. Then, 200 μL of magnetic beads were washed three times with 300 μL of borate buffer 100 mM pH 9.5 in a 2 mL Eppendorf. The magnetic beads were then resuspended by adding 400 μL of different concentrations of AFB1-OVA in borate buffer (100 mM pH 9.5). Next, 200 μL of borate buffer 100 mM pH 9.5 containing 3 M ammonium sulfate was added and the mixture was incubated overnight at 37 °C while shaking with slow tilt rotation at 30 rpm in the dark. After that, the modified magnetic beads were washed three times in PBST 10 mM, pH 7.5, containing 0.5% (w/v) BSA, and incubated overnight at room temperature while shaking with slow tilt rotation at 30 rpm in the dark. Finally, the magnetic beads were resuspended in 1 mL of PBST, 0.1% (w/v) BSA, and kept at 4 °C in the fridge. According to the provider, the covalently modified magnetic beads with AFB1-OVA were stable for at least three months when stored at 4 °C.

2.3. Modification of the SPE with CB

The SPE was modified with CB as previously described [40]. A mixture of 3 mg/mL CB in DMF: H_2O (1:1, v/v) was prepared. The mixture was sonicated using a Hielscher's UP 200ST until homogenously dispersed, with an amplitude of 80%, a pulse of 30%, and energy of 3800 W/mL. To modify the SPE, 1 μL of the carbon black dispersion was drop cast on the working electrode area using a Biodot XYZ3210 dispenser. The modified electrodes were dried in a humidity chamber (65% humidity; 23–25 °C; overnight) to ensure uniform coverage and avoid coffee-ring formation. We reported previously the inter-day and intra-day stability of modified electrodes with CB using the same protocol [41]. The electrochemical stability of CB-modified electrodes was analyzed using CV and EIS methods. The measurements were performed directly after modification (intra-day) and after 7, 20, 60, 90, and 180 days of storage under vacuum (inter-day). Based on EIS analysis, the variance in electron transfer resistance after different storage times was lower for CB-modified electrodes compared to the bare electrodes. Also, the internal variance in anodic peak currents in CV analysis was reduced after the modification of SPE with CB. Based on CV and EIS analysis, the storage stability of electrodes after modification with CB was increased for up to at least six months.

2.4. Electrochemical characterization of SPE-CB

Electrochemical characterization of SPE-CB was performed using CV and EIS methods. The CV and EIS measurements were performed in 5 mM $[Fe(CN)_6]^{3-/4-}$ in MilliQ water pH 6.5 in presence of 0.1 M KCl at room temperature. In CV, the potential was scanned from −0.3 to 0.6 V with a scan rate of 0.1 V/s and a step potential of 0.01 V for 2 cycles using 3 electrodes. EIS measurements were performed at an applied potential of 0 V versus V_{OCP}, a frequency range of 0.1 Hz–100 kHz, and an amplitude of 10 mV using 3 electrodes.

2.5. Design and fabrication of a micro-machined magnetic holder

An external magnet was used for the immobilization of magnetic beads on the SPE working electrode. A micro-machined magnetic holder provided precise magnet placement under the working electrode. The magnetic holder was designed using Solidworks 2018 and fabricated with CNC machining (supporting information S1). The top part was a 1 mm thick polycarbonate, and the bottom part was a 5 mm thick polymethyl methacrylate substrate (supporting information S1). The top and bottom parts were milled with a feed rate X/Y/Z of 600 mm/min, and at a rotation speed of 3000 rpm.

2.6. Magneto-immunoassay

To perform the competitive assay, 100 μL of the magnetic beads conjugated with AFB1-OVA (MB-OVA-AFB1) solution was incubated with the AFB1-mAb and with different concentrations of aflatoxin B1 in reagent dilution buffer for 1 h at room temperature with a continuous

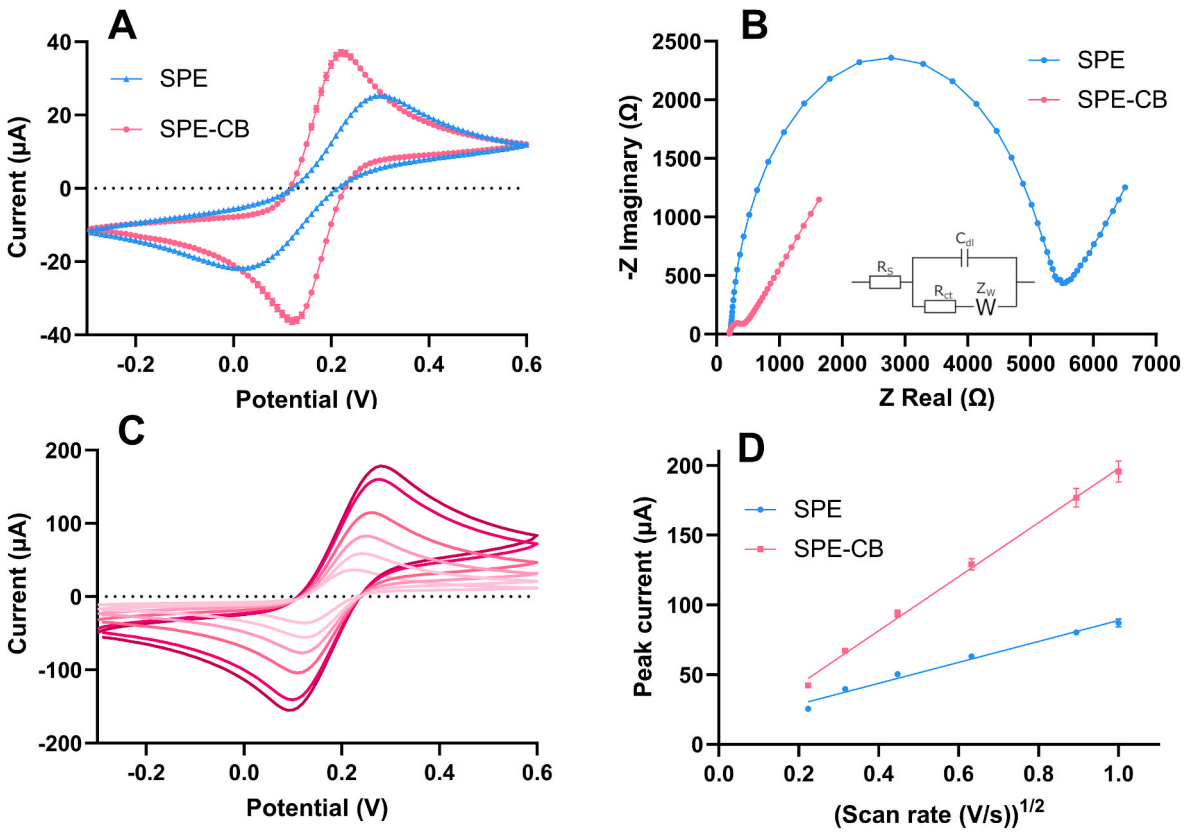

Fig. 1. Electrochemical characterization of CB modified electrode (SPE-CB) in 5 mM $[Fe(CN)_6]^{3-/4-}$ containing 0.1 M KCl solution. A) Cyclic voltammograms SPE-CB and SPE electrodes. After modification of electrode with CB, the current peaks increased, and peak-to-peak potential difference decreased which indicated an increase in both surface area and electron transfer rate on the modified electrode. B) Nyquist plots on SPE-CB and SPE electrodes. The semicircle diameter corresponding to charge transfer resistance of electrode decreased almost 30 times after modification with carbon black nanomaterial, indicating higher electron transfer and better electrochemical performance of SPE-CB. C) Cyclic voltammogramms on SPE-CB at increasing scan rate from 0.05 to 1 V/s. Lower scan rate was indicated with light color and an increase in scan rate was shown by increasing darkness of color. The current peaks increased with increasing scan rates as expected for a diffusion limited electron transfer D) The plot shows the linear regression of peak current versus square root of the scan rate used for the calculation of SPE and SPE-CB electroactive surface area. (For interpretation of the references to color in this figure legend, the reader is referred to the Web version of this article.)

slow tilting rotation. Then, the Eppendorf tubes were put on the magnetic rack for 2 min and the supernatant was removed. The magnetic beads were then resuspended in 1 mL of the washing buffer and placed back on the magnetic rack for 2 min after which the supernatant was removed again. The washing step was repeated three times. Next, 100 μL of the HRP-pAb in reagent dilution buffer was added to Eppendorf tubes and incubated for 30 min at room temperature with slow tilt rotation. The previously described washing step was repeated three times.

2.7. Electrochemical measurements

For electrochemical measurement, magnetic beads were resuspended in 40 μL of citrate-phosphate buffer (0.05 M, pH 5). The SPE was fixed in the magnetic holder with an external magnet under the working electrode. Then, 10 μL of the magnetic beads' suspension was dropped on the working electrode. Immediately after the addition of the magnetic beads, 35 μL of the substrate solution (1 mM HQ, 1 mM H_2O_2 in citrate-phosphate buffer) was added to the cell and mixed carefully so that the SPE surface was covered. After 2 min of reaction time, the chronoamperometric measurements were performed at −0.2 V at an interval time of 0.1 s for 30 s. The reaction time was chosen based on the previously reported protocols for amperometry measurement of the HRP/HQ/H_2O_2 system and the reaction mechanism [42–44]. During the 2 min reaction time, the HRP catalyzes the oxidation of hydroquinone (HQ) by hydrogen peroxide (H_2O_2) producing benzoquinone (BQ). Then, the current produced by the reduction of BQ was measured by the chronoamperometry method.

The currents generated from the reaction after 30 s were plotted in front of aflatoxin B1 concentration. The standard curves were fitted to a four-parameter dose-response curve with variable slope based on the equation below:

$$Y = \left(\frac{A - B}{\left[1 + 10^{(logIC50 - X)D}\right]}\right) + B \quad (1)$$

A is the maximal current, B is the minimum current, IC50 is the concentration producing 50% of the maximal current, and D is the slope at the inflection point of the sigmoidal curve. Unless otherwise indicated, the data presented correspond to the average of at least 3 replicates.

2.8. Aflatoxin B1 extraction procedure

To extract the aflatoxin B1 from cereal samples, 10 mL of extraction solvent (80% methanol solution) was added to 5 g of finely grounded samples. The mixture was vortexed for 15 min and then left to settle down for 2 min. Next, the supernatant was filtered with a 2 μm syringe filter. The extract was used for measurements after 10 times dilution in reagent dilution buffer with no further clean-up. Based on the extraction procedure, the EU MRL for aflatoxin B1 of 2 μg/kg corresponds to an in-assay concentration of 100 pg/mL. Using the same extraction procedure, the effect of potential interfering aflatoxins B2, G1, and G2 on the selectivity of the assay was also evaluated.

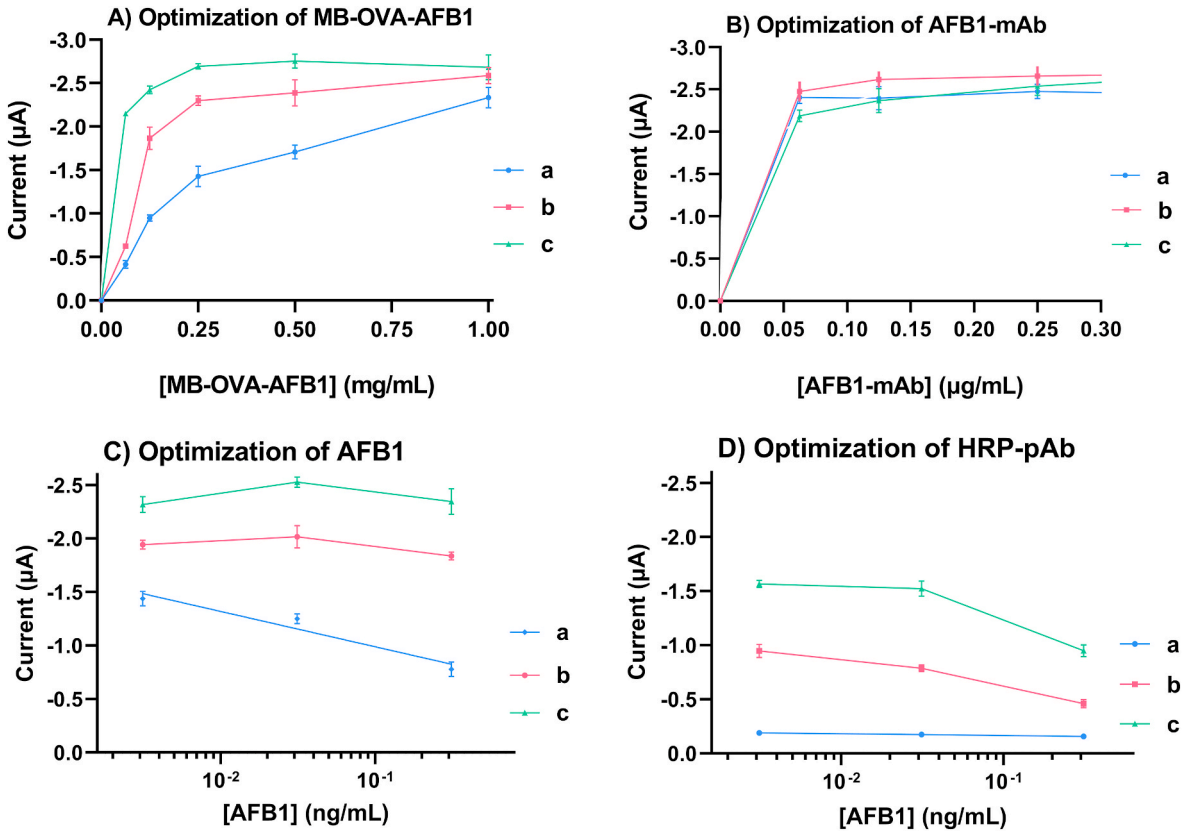

Fig. 2. Optimization of the immunoreagents concentrations MB-OVA-AFB1, AFB1-mAb, AFB1-OVA density on magnetic beads, and HRP-pAb. A) The non-competitive binding curves of AFB1-mAb to increasing concentration of MB-OVA-AFB1 at 3 different AFB1-OVA densities (a: 2.27, b: 4.55, c: 9.10×10^{-12} mol/μm^2) in the absence of free aflatoxin B1. The optimum concentration of MB-OVA-AFB1 producing 90% of saturating signal were 0.7, 0.4, and 0.1 mg/mL at AFB1-OVA densities of a, b, and c, respectively. The magnetic beads with the lowest density of AFB1-OVA, batch a, required the highest concentration of MB-OVA-AFB1 to reach the saturation signal. B) The non-competitive binding curves of the optimum MB-OVA-AFB1 obtained in A to increasing concentration of AFB1-mAb in the absence of free aflatoxin B1. The optimum concentration of AFB1-mAb producing 90% of saturating signal were 0.015, 0.05, and 0.2 μg/mL for a, b, and c respectively. C) The competitive binding curves of aflatoxin B1 using optimum concentrations of AFB1-mAb and MB-OVA-AFB1 with AFB1-OVA densities of a, b, and c. The magnetic beads with the lowest density of AFB1-OVA (a) distinguished the aflatoxin B1 concentrations at 0.3, 0.03, and 0.003 ng/mL. D) The competitive binding curves of aflatoxin B1 using optimum concentrations of AFB1-mAb and MB-OVA-AFB1 with AFB1-OVA density of 2.27×10^{-12} nmol/μm^2 (a) with different HRP- pAb concentration 1/1500 (a), 1/1000 (b), and 1/500 (c) dilutions of stock solution 0.8 mg/mL. The assay distinguished aflatoxin B1 concentrations of 0.3, 0.03, and 0.003 ng/mL using HRP- pAb dilution 1/1000 (80 μg/mL).The standard deviations correspond to measurements performed using three different SPE-CB electrodes.

2.9. Validation study

In-house validation was performed based on the EU commission regulation (EU) No 519/2014. The protocol included 20 blank samples of cereals (non-contaminated) certified by the HPLC-MS and ELISA methods (supporting information S2). The 20 blank samples were spiked with aflatoxin B1 stock solution at the screening target concentration which was set at 2 μg/kg based on the EU Commission Regulation (EC) No. 1881/2006. All samples were tested using the magneto-immunosensor to detect aflatoxin B1. Each sample was tested in triplicates. The samples were analyzed under intermediate precision conditions over five different days in random blind order.

2.10. Development of the smartphone application: AflaESense

The electrochemical output data from the magneto-immunosensor is in the format of a graph of the current signal over time. To determine the aflatoxin B1 concentration in the sample, the data should be analyzed by an expert to extract the average current value, interpolate the aflatoxin B1 concentration using the calibration curve, and determine the level of contamination compared to the EU MRL. To overcome the need for expertise to perform this analysis, we developed a smartphone application to automate the data analysis and provide a non-expert and user-friendly output. Thus, an open-source Android application was developed for the miniaturized potentiostat, Sensit Smart using a PalmSense software development kit. The codes were written in Visual Studio.NET using Xamarin and C# programming language. The PalmSens.Core.dll open-source wrapper was utilized for basic functions such as connecting to the device, running the measurements, defining the chronoamperometry method parameters, and logging the data. The user interface forms, and data analysis codes were also written using Xamarin and C# programming language. The open-source application, which we called AflaESense, can be downloaded from AflaESens.app.

https://drive.google.com/file/d/1Mv0SHkmWrd-DITKYRlSEGEGS0kcGOMAr/view.

3. Results & discussion

3.1. Electrochemical characterization of SPE-CB

To improve the electrochemical performance of bare SPE electrodes for the detection of aflatoxin B1, CB coating was used to modify the SPE surface as a signal amplification strategy owing to its low cost, high reproducibility, and storage stability [41]. We characterized SPE-CB electrodes by CV and EIS to investigate the effect of CB on the electrochemical performance of modified electrodes.

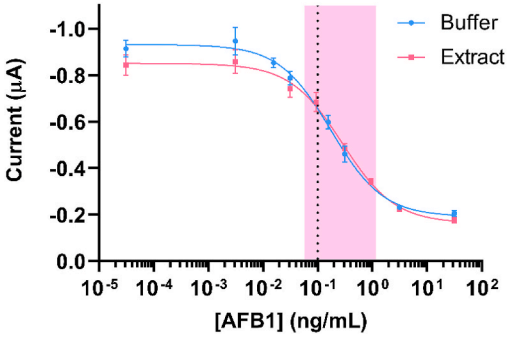

Analytical parameters	Buffer	Extract
LOD (pg/mL)	13	24
Linear range	33-735	57-1557
IC50 (pg/mL)	156.5	257.1
Hillslope	-0.90	-0.92
R square	0.99	0.99
Mean RSD	3.74%	4.01%

Fig. 3. Detection of different concentrations of aflatoxin B1 in buffer and corn extract. The assay was based on an indirect competitive immunoassay. The current response decreased as aflatoxin B1 concentration increased. The dashed line indicates the EU MRL for aflatoxin B1 (2 μg/kg), which lies in the assay dynamic range in both buffer and corn extract. The highlighted area of the curve in pink shows the linear range of the magneto-immunoassay in extract producing 20–80% of the maximum signal. The binding curve in the extract is the average of three independent calibrations over three days, where each concentration was measured on three different SPE-CB electrodes. Low RSD values in the buffer and extract indicated high reproducibility of the assay. (For interpretation of the references to color in this figure legend, the reader is referred to the Web version of this article.)

To characterize the effect of CB modification on the electrochemical performance of the SPE electrode, we analyzed the electron transfer rate on the surface of SPE with and without CB coating with CV. In the resulting cyclic voltammograms, the anodic and cathodic peak currents of the $[Fe(CN)_6]^{3-/4-}$ standard solution depends on the surface area of the electrode and electron transfer rate, while the peak-to-peak potential difference qualitatively indicates the electron transfer rate. Based on CV analysis, anodic peak current using SPE-CB was 1.5 times higher than SPE, and the peak-to-peak potential difference using SPE-CB was 2.5 times lower than SPE indicating an increase in both the electroactive surface area and electron transfer rate after modification of the electrode with CB (Fig. 1A). The peak current increased by increasing the scan rate from 0.05 to 1 V/s in $[Fe(CN)_6]^{3-/4-}$ standard solution for both unmodified and modified electrodes (Fig. 1C) [45]. Based on the relationship between peak current and scan rate, the electroactive surface area was calculated with the Randles-Sevcik equation; it increased from 0.027 ± 0.001 to 0.056 ± 0.007 cm^2 after modifying the electrodes with CB (Fig. 1D) (see supporting information S3 for calculations).

To characterize the influence of CB modification on the electrochemical performance of the SPE electrodes, we analyzed the interfacial electron transfer on the SPE with and without CB coating with EIS. The semicircle diameter in the Nyquist plot of impedance spectra corresponds to the charge transfer resistance on the electrode surface, which in turn affects the electron transfer rate [45]. The Nyquist plot in Fig. 1B shows the impedance spectra of SPE-CB and SPE in $[Fe(CN)_6]^{3-/4-}$ standard solution over a frequency range of 0.1–1000 kHz. The spectra were fitted to a Randles circuit (Fig. 1B inset) and consisted of the electrolyte resistance (Rs), interfacial charge transfer resistance (R_{ct}), the analytes diffusion or Warburg impedance (Zw), and double-layer capacitance (Cdl) (see supporting information S4 for detailed parameters of the fit). The electron transfer resistance (R_{ct}) on the SPE-CB decreased 30 times from 4596.7 to 164.8 Ω, resulting in a higher electron transfer rate. The results of this impedance analysis were in agreement with the cyclic voltammetry results and previous reports on the electrochemical characteristics of CB-modified electrodes [42,46]. These data confirm the signal amplification and better electrochemical performance of SPE after modification with CB.

3.2. Optimization of the magneto-immunosensor

Having established the effective signal amplification and better electrochemical performance of using SPE-CB electrodes, the analytical performance of the magneto-immunosensor for detecting aflatoxin B1 was optimized using SPE-CB electrodes. The analytical performance of a magneto-immunosensor as a heterogeneous binding assay depends on the antigen density of the magnetic beads, the concentrations of beads, and the concentration of antibodies [47]. The magneto-immunosensor working principle was based on indirect competitive ELISA. First, aflatoxin B1 in the sample competed with AFB1-OVA on magnetic beads (MB-OVA-AFB1) for binding to a certain number of antibodies (AFB1--mAb). After separating the magnetic beads, HRP-pAb is bound to the AFB1-mAb on magnetic beads. Then, magnetic beads were immobilized on the electrode using an external magnet underneath the electrode. The current generated from the HRP reaction with the substrate (HQ/H_2O_2) was inversely proportional to aflatoxin B1 concentration. Higher concentrations of aflatoxin B1 in the sample resulted in a lower amount of bound HRP-pAb to the magnetic beads and a lower current signal.

The concentrations of MB-OVA-AFB1, AFB1-mAb, and HRP-pAb were optimized for detecting aflatoxin B1 by using different densities of AFB1-OVA covalently immobilized on magnetic beads $2.27{\cdot}10^{-12}$, $4.55{\cdot}10^{-12}$, and $9.10{\cdot}10^{-12}$ mol/μm^2 labeled as a, b, and c respectively (see supporting information S5 for calculations). First, the MB-OVA-AFB1 and AFB1-mAb were optimized using a non-competitive immunoassay in the absence of aflatoxin B1. Then, the HRP-pAb and the magnetic-based density were optimized by competitive binding in the presence of aflatoxin B1 [48].

A non-competitive titration of MB-OVA-AFB1 with a constant amount of AFB1-mAb (0.25 μg/mL) and HRP-pAb (160 μg/mL), concentrations selected based on ELISA assay results (supporting information S6), as performed (Fig. 2A). The optimum concentrations of MB-OVA-AFB1 observed to saturate the signal by 90% were 0.7, 0.4, and 0.1 mg/mL of beads, and AFB1-OVA densities of 2.27, 4.55, and $9.10{\cdot}10^{-12}$ mol/μm^2 (a, b, and c) respectively. The use of a higher number of beads produced a saturated current signal at a lower AFB1-OVA density. The optimum MB-OVA-AFB1 concentrations were then used for AFB1-mAb optimization. The optimum AFB1-mAb concentrations producing 90% of saturation signal were 0.015, 0.05, and 0.2 μg/mL at AFB1-OVA with densities 2.27, 4.55, and $9.10{\cdot}10^{-12}$ mol/μm^2 (a, b, and c), respectively (Fig. 2B). At this step, the lowest AFB1-mAb required to saturate the signal was observed using the highest concentration of MB-OVA-AFB1 with the lowest OVA-AFB1 density (batch a, Fig. 2B).

In the next step, the density of the magnetic beads was optimized using the competitive binding of aflatoxin B1 to AFB1-mAb, with a constant concentration of HRP-pAb. Only the use of MB-OVA-AFB1 with the lowest density of AFB1-OVA (batch a, Fig. 2C) allowed for distinguishing the low levels of aflatoxin B1 concentrations in the range of 0.3, 0.03, and 0.003 ng/mL. This may be due to better binding kinetics and a higher probability of binding when using a higher number of beads with a lower density of AFB1-OVA. Moreover, the combination of a higher number of beads and a lower density of AFB1-OVA resulted in a lower number of final immunocomplexes on a single bead. Thus, the signal variability due to the loss of a few beads was minimized, improving reproducibility. Finally, the HRP-pAb concentration was optimized using MB-OVA-AFB1 with $2.27{\cdot}10^{-12}$ mol/μm^2 of AFB1-OVA. Using an HRP-pAb dilution of 1/1000 (80 μg/mL) (Fig. 2D, red) led to the determination of aflatoxin B1 concentrations at 0.3, 0.03, and 0.003 ng/mL. While using a higher concentration of HRP-pAb (1/500 dilution)

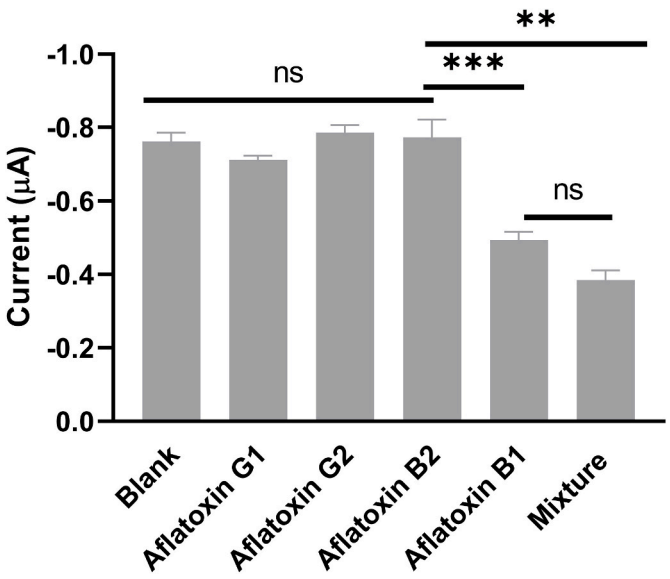

Fig. 4. Selectivity of developed magneto-immunosensor for aflatoxin B1 detection. As a control experiment, the non-contaminated corn sample (blank) extract was spiked with 4 μg/kg of aflatoxins G1, G2, and B2, 0.2 ng/mL in assay concentration. One-way ANOVA analysis of the assay response showed no significant (ns) difference between blank, aflatoxin G1, G2, and B2 responses while there was a significant difference between blank and aflatoxin B1 at 2 μg/kg, 0.1 ng/mL in-assay concentration and the mixture of aflatoxins responses (** equals $p < 0.01$ and ***$p < 0.001$). The mixture contained each aflatoxin G1, G2, and B2 at 4 μg/kg and aflatoxin B1 at 2 μg/kg. The standard deviations correspond to the measurement using three SPE-CB electrodes.

led to a steeper difference between 0.3 and 0.03 ng/mL of aflatoxin B1 concentrations, it was not possible to distinguish between lower concentrations of 0.03 and 0.003 ng/mL of aflatoxin B1 with these conditions. Thus, the HRP- pAb at 1/1000 dilution was chosen as the optimum concentration.

3.3. Analytical performance of the magneto-immunosensor

The analytical performance of magneto-immunosensor for detection of aflatoxin B1 has been evaluated using the optimum parameters of AFB1-OVA density of $2.27 \cdot 10^{-12}$ mol/μm^2 on magnetic beads, MB-OVA-AFB1 concentration of 0.7 mg/mL, AFB1-mAb concentration of 0.015 μg/mL, and HRP-pAb concentration of 80 μg/mL. The calibration curves in Fig. 3 show the sigmoidal curves of aflatoxin B1 antibody binding to different concentrations of aflatoxin B1 in buffer and non-contaminated corn extract. The nonlinear fit of binding curves was performed based on equation (1) (see Material & methods, 2.5), using four parameters log inhibitor vs current response with variable slope at a 95% confidence interval. Limit of detection (LOD), half-maximal inhibitory concentration (IC50), and linear range of the assay were calculated as the concentration of aflatoxin B1 which gives 90%, 50%, and 20–80% of the maximum current signal produced by the binding reaction, respectively. LOD values were estimated to be as low as 13 and 24 pg/mL for buffer and corn sample extract, respectively. The EU MRL for aflatoxin B1 of 2 μg/kg corresponding to an in-assay concentration of 100 pg/mL was covered in the assay linear range both in buffer and corn extract. The inter-assay precision was also investigated by testing the same corn sample extract with a magneto-immunosensor under the same experimental conditions over three days. The non-contaminated extracts were spiked with different concentrations of aflatoxin B1 from 30 to 0.003 ng/mL. Mean relative standard deviations of the assay were 3.7% and 4.0% in buffer and three non-contaminated corn extracts spiked with aflatoxin B1 measured over three days, respectively, indicating high reproducibility of the assay. The relative standard deviation for each aflatoxin B1 concentration was obtained using three different SPE-CB electrodes.

Selectivity of the magneto-immunoassay was evaluated by performing a control experiment in the presence of the most prevalent potential interfering aflatoxins: aflatoxin B2, aflatoxin G1, and aflatoxin G2, all commonly found in corn extract. The non-contaminated corn extract was spiked with aflatoxin B1 at 2 μg/kg, which corresponds in the assay to a concentration of 0.1 ng/mL, and aflatoxin B2, G1, and G2 at 4 μg/kg (which corresponds in the assay to a concentration of 0.2 ng/mL, the EU MRL for total aflatoxins B1, B2, G1, and G2). Based on one-way ANOVA analysis, no significant differences between the blank signal and the magneto-immunosensor signals for aflatoxin G1, G2, and B2 were observed with p values of 0.38, 0.96, and >0.99 respectively (Fig. 4). There were significant differences when the blank signal was compared with aflatoxin B1 and the mixture signals with p values of 0.0009 and 0.0026, respectively, while there was no significant difference between aflatoxin B1 and the mixture signals with a p-value of 0.086. Therefore, the magneto-immunosensor demonstrated good selectivity to detect aflatoxin B1 in the cereals extract at the studied concentrations.

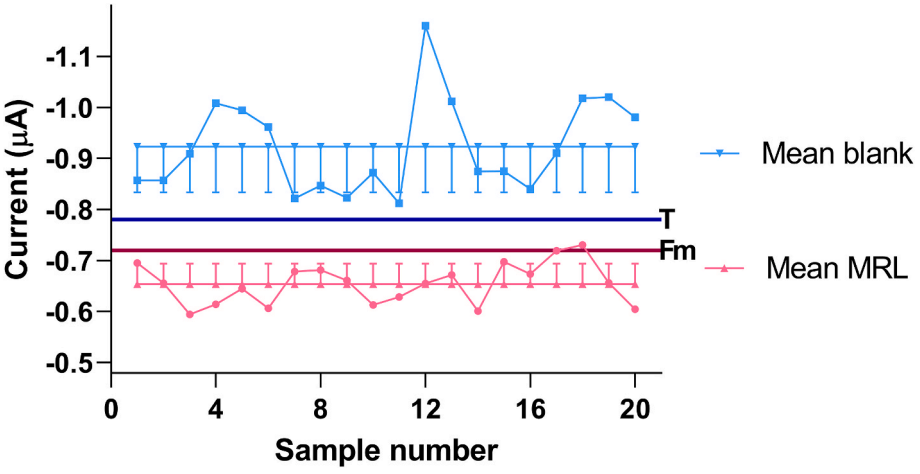

Fig. 5. In-house validation of the magneto-immunoassay for detection of aflatoxin B1. Any sample producing a signal greater than the cut-off value (Fm −0.72 μA) is positive or suspect and any sample producing a signal less than the threshold value (T −0.77 μA) is negative or non-contaminated. The standard deviations of mean blank and mean MRL is the average standard deviation of 20 measurements, each performed in triplicates using three SPE-CB electrodes.

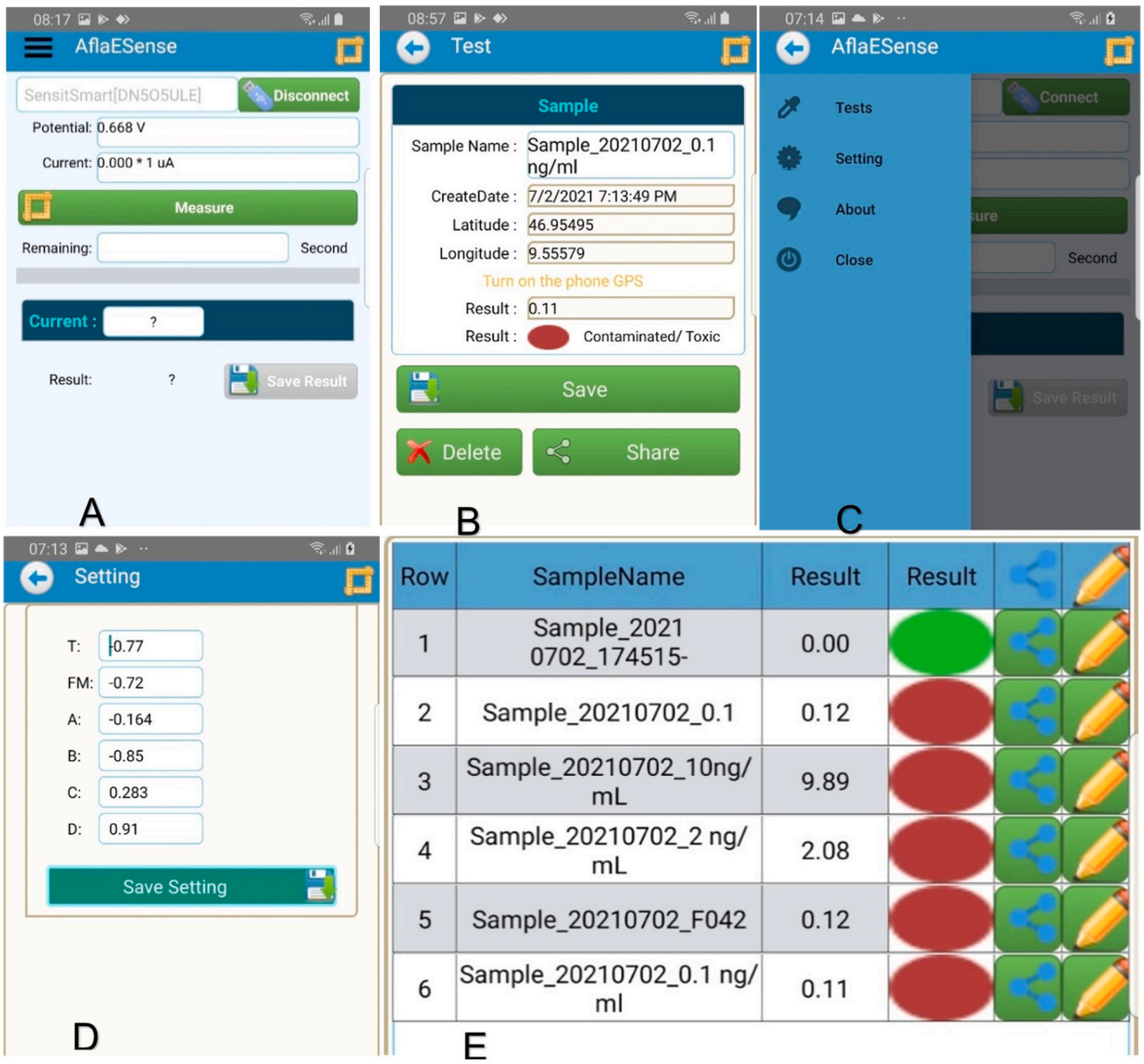

Fig. 6. AflaESense user interface. A) the main page includes the device connection status, running the measurement, reaction time progress bar, measured current value, estimated result, and save result option; B) the test page shows the sample name (editable), timestamp (date), location (latitude and longitude), the numerical value of the result, traffic light type indication of result, save, share, and delete option; C) menu includes tests table, setting, about, and close options; D) setting page includes threshold (T), cut-off factor (Fm), and calibration parameters based on equation (1), the maximal current (A), the minimum current (B), the concentration producing 50% of the maximal current (IC50), and the slope at the inflection point of the sigmoidal curve (D); E) AflaESense result page for real sample analysis. The screenshot shows the results for a blank sample (row 1) spiked samples at 0.1, 2, and 10 ng/mL (rows 2, 3, 4, and 6), and a naturally contaminated sample at 0.15 ng/mL (row 5).

3.4. Validation study

Having accomplished the good analytical performance of magneto-immunosensor for detection of aflatoxin B1 with a low LOD of 24 pg/mL and mean RSD of 4.01%, the magneto-immunosensor applicability as an aflatoxin B1 screening test for cereals was further investigated. For this purpose, an in-house validation study based on EU guidelines (EU commission regulation (EU) No 519/20149) for screening tests was performed using 20 certified non-contaminated cereal samples (blank samples). After extraction, all non-contaminated samples were spiked with aflatoxin B1 at a screening target concentration of 2 μg/kg, corresponding to 0.1 ng/ml in assay concentration (EU MRL for aflatoxin B1). The measurements were performed over five days in triplicates under intermediate precision conditions, i.e. keeping all the experimental conditions constant with the day of experiment as the only variable. The threshold (T) and the cut-off factor (Fm) values determine the decision limit for negative and positive samples, respectively. They were determined using the equations below:

$$T = B - 1.64\ \ SDB \quad (2)$$

(EU commission regulation (EU) No 519/2014)

$$Fm = M + 1.64\ \ SDM \quad (3)$$

(EU commission regulation (EU) No 519/2014).

B is the mean and SDB is the mean relative standard deviation of the blank samples signal. M is the mean and SDM is the mean relative standard deviation of the spiked samples signal. The current values for B, SDB, M, and SDM were -0.92 ± 0.09 μA, -0.65 ± 0.04 μA, respectively. Then, the Fm and T values were -0.72 and -0.77 μA, respectively. Based on the validation experiment, the cut-off factor (Fm) was smaller than the threshold value, indicating a detection capability (CCβ) less than or equal to 2 μg/kg, a false-negative rate lower than 5%, and a false-positive rate lower than 5% (Fig. 5). Any sample producing a signal greater than the cut-off value (Fm -0.72 μA) is considered positive or suspect and any sample producing a signal less than the threshold value (T -0.77 μA) is considered negative or non-contaminated within the 5%

Table 1
Summary of data shown on the result page of AflaESense. The reported values by AflaESense are in close agreement with known concentrations with recovery values between 80 and 120%.

Sample name	AFB1 present (ng/mL)	AFB1 measured (ng/mL)	Recovery %
2021_0702_174515	0.0	0.0	100
2021_0702_0.1	0.1	0.12	120
2021_0702_10 ng/mL	10	9.89	99
2021_0702_2 ng/mL	2	2.08	104
2021_0702_F042	0.15	0.12	80
2021_0702_0.1 ng/mL	0.1	0.11	110

false-positive and false-negative rates.

3.5. Real sample analysis using a smartphone

The Android application AflaESense was developed to provide a user-friendly interface for non-expert users (Fig. 6). AflaESens enables the user to perform the electrochemical measurement of the magneto-immunosensor on a commercial miniaturized potentiostat (Sensit Smart, Palmsens, Netherlands) connected to the phone via a USB. AflaESense was used as the measurement interface to detect aflatoxin B1 in spiked corn samples containing 0.1, 2, and 10 ng/mL aflatoxin B1 and a naturally contaminated sample, F042, with 0.15 ng aflatoxin B1/mL. After performing the magneto-immunoassay, the magnetic beads were transferred to the SPE-CB electrode connected to the Sensit Smart device. Then the substrate was added, and the measurement was started by pressing the measure button on the phone (Fig. 6A). The current signal was measured after 2 min of reaction time. The data was analyzed automatically based on the validation study and calibration curve in the corn extract. As shown in Table 1, the reported result with AflaESense was in close agreement with the spiked concentrations ($r^2 = 0.99$) with recovery values between 80 and 120%. These recovery values were in the acceptable range based on the EU guideline for screening tests for aflatoxin B1 (EU commission regulation (EU) No 519/2014), which demonstrated the AflaESense capability in performing the measurement and data analysis. The result sheet including a timestamp, GPS location, and sample name can be saved on the phone's internal storage or shared via other applications (email, Bluetooth, WhatsApp …).

Quantitative results in the ng/mL range produced by AflaESense are similar to the quantification range of previously reported smartphone-based applications such as point-of-care testing systems for neuron-specific enolase and PfHRP2 detection [49,50]. Smartphone-based applications reported in previous studies are mostly designed for in-house potentiostats with smartphone connectivity, reducing costs relative to using AflaESense [51]. However, the use of a commercially available smartphone potentiostat, Sensit Smart, is advantageous due to its wide availability.

4. Conclusion

Applicability and user-friendliness are key features of point-of-need biosensing devices but are often overlooked in research. In this study, we developed a highly sensitive and reproducible magneto-immunosensor for point-of-need detection of aflatoxin B1 by non-expert users. The LOD values of 13 and 24 pg/mL and mean relative standard deviations (RSD) of 3.7% and 4.0% were obtained in the buffer and extract, respectively. The sensor can be used to detect aflatoxin B1 at a concentration of 2 μg/kg, the EU MRL (in-assay concentration of 100 pg/mL), and it was validated to have a CCβ lower or equal to this value. The false-positive and false-negative rates were less than 5%, meeting regulatory requirements for food safety testing. Finally, AflaESense, a user-friendly android application, was designed based on validation results such as threshold and cut-off values. AflaESense, combined with a commercial miniaturized potentiostat connected to the smartphone was effectively used to accurately evaluate various samples that were either not contaminated or spiked with increasing amounts of aflatoxin B1 (0.1, 10, and 20 ng/mL), as well as naturally contaminated samples. The results were also visualized in a simple to interpret, traffic-light-type format; red for contaminated samples and green for non-contaminated samples minimizing the need for user training and cumbersome data analysis. Thus, the method described here combines a CB-coated electrochemical immunosensor, a miniaturized potentiostat, and a customized smartphone App, demonstrating an innovative proof of concept for point-of-need food safety testing for aflatoxin B1 by non-experts. For the widespread application of such devices, further work is needed to address the integration and automation of multiple sample preparation steps such as extraction and washing, which are critical for reliable results.

Funding

This project has received funding from the European Union's Horizon 2020 research and innovation program under the Marie Sklodowska-Curie grant agreement No 720325.

CRediT authorship contribution statement

Safiye Jafari: Conceptualization, design and performing experiments, data analysis, Software, development, Writing – original draft, revision, and editing. **Loïc Burr:** magnetic holder design and fabrication, experimental design, review, and editing. **Davide Migliorelli:** experiment design, administration. **Roger Galve:** experimental design, review, and editing. **M.-Pilar Marco:** review, and editing. **Katrina Campbell:** providing the AFB1-OVA conjugate, review, and editing. **Chris Elliott:** providing the AFB1-mAb and blank samples, review, and editing. **Michele Suman:** providing the blank samples. **Shana J. Sturla:** Supervision, writing. **Silvia Generelli:** Supervision, writing.

Declaration of competing interest

The authors declare that they have no known competing financial interests or personal relationships that could have appeared to influence the work reported in this paper.

Data availability

Data will be made available on request.

Acknowledgment

We thank Prof. Michel Nielen ((Wageningen Food Safety Research (WFSR), part of Wageningen University & Research, Wageningen, The Netherlands) for kindly providing the certified non-contaminated (blank) and naturally contaminated samples.

Appendix A. Supplementary data

Supplementary data to this article can be found online at https://doi.org/10.1016/j.aca.2022.340118.

References

[1] B.R. Rushing, M.I. Selim, Aflatoxin B1: a review on metabolism, toxicity, occurrence in food, occupational exposure, and detoxification methods, Food Chem. Toxicol. 124 (2019) 81–100, https://doi.org/10.1016/j.fct.2018.11.047.
[2] A.B. Engin, A. Engin, DNA damage checkpoint response to aflatoxin B1, Environ. Toxicol. Pharmacol. 65 (2019) 90–96, https://doi.org/10.1016/j.etap.2018.12.006.
[3] R.G. Ferreira, M.V. Cardoso, K.M. de Souza Furtado, K.M.M. Espíndola, R. P. Amorim, M.C. Monteiro, Epigenetic alterations caused by aflatoxin b1: a public

health risk in the induction of hepatocellular carcinoma, Transl. Res. 204 (2019) 51–71, https://doi.org/10.1016/j.trsl.2018.09.001.
[4] S. García-Fonseca, A. Ballesteros-Gómez, S. Rubio, Restricted access supramolecular solvents for sample treatment in enzyme-linked immuno-sorbent assay of mycotoxins in food, Anal. Chim. Acta 935 (2016) 129–135, https://doi.org/10.1016/j.aca.2016.06.042.
[5] Commission of the European Communities, Amending Regulation (EC) No 1881/2006 as regards maximum levels for polycyclic aromatic hydrocarbons in foodstuffs, Off. J. Eur. Union (2011) 4–8. No. L215/4.
[6] Commission of the European Communities, Commission Regulation (EU) No 165/2010 of 26 February 2010 amending Regulation (EC) No 1881/2006 setting maximum levels for certain contaminants in foodstuffs as regards aflatoxins, Off. J. Eur. Union L 50/8 (2010) 5.
[7] Commission of the European Communities, Commission Regulation (EC) No 1152/2009 of 27 November 2009 imposing special conditions governing the import of certain foodstuffs from certain third countries due to contamination risk by aflatoxins and repealing Decision 2006/504/EC, Off. J. Eur. Union 313 (2009) 40–49.
[8] Commission of the European Communities, Commission Regulation (EC) No 1881/2006 of 19 December 2006 setting maximum levels for certain contaminants in foodstuffs, Off. J. Eur. Union (2006) 5–24.
[9] Efsa, RASFF portal | food safety [WWW Document]. URL, https://webgate.ec.europa.eu/rasff-window/screen/search, 2020, 3.1.20.
[10] D. Schrenk, M. Bignami, L. Bodin, J.K. Chipman, J. del Mazo, B. Grasl-Kraupp, C. Hogstrand, L. Hoogenboom, Ron, J. Leblanc, C.S. Nebbia, E. Nielsen, E. Ntzani, A. Petersen, S. Sand, T. Schwerdtle, C. Vleminckx, D. Marko, I.P. Oswald, A. Piersma, M. Routledge, J. Schlatter, K. Baert, P. Gergelova, H. Wallace, Risk assessment of aflatoxins in food, EFSA J. 18 (2020), https://doi.org/10.2903/j.efsa.2020.6040.
[11] A.M.A. Alsharif, Y.M. Choo, G.H. Tan, Detection of five mycotoxins in different food matrices in the malaysian market by using validated liquid chromatography electrospray ionization triple quadrupole mass spectrometry, Toxins 11 (2019), https://doi.org/10.3390/toxins11040196.
[12] T. He, T. Zhou, Y. Wan, T. Tan, A simple strategy based on deep eutectic solvent for determination of aflatoxins in rice samples, Food Anal. Methods 13 (2020) 542–550, https://doi.org/10.1007/s12161-019-01665-7.
[13] P. Jedziniak, Ł. Panasiuk, K. Pietruszka, A. Posyniak, Multiple mycotoxins analysis in animal feed with LC-MS/MS: comparison of extract dilution and immunoaffinity clean-up, J. Separ. Sci. 42 (2019) 1240–1247, https://doi.org/10.1002/jssc.201801113.
[14] L. Yu, F. Ma, L. Zhang, P. Li, Determination of aflatoxin B1 and B2 in vegetable oils using Fe3O4/rGO magnetic solid phase extraction coupled with high-performance liquid chromatography fluorescence with post-column photochemical derivatization, Toxins 11 (11) (2019) 621, https://doi.org/10.3390/toxins11110621.
[15] A. Ainla, M.P.S. Mousavi, M. Tsaloglou, J. Redston, J.G. Bell, M.T. Fernández-Abedul, G.M. Whitesides, Open-source potentiostat for wireless electrochemical detection with smartphones, Anal. Chem. 90 (2018) 6240–6246, https://doi.org/10.1021/acs.analchem.8b00850.
[16] M.D.M. Dryden, A.R. Wheeler, DStat: a versatile, open-source potentiostat for electroanalysis and integration, PLoS One 10 (2015), e0140349, https://doi.org/10.1371/journal.pone.0140349.
[17] S.C. Kim, U.M. Jalal, S.B. Im, S. Ko, J.S. Shim, A smartphone-based optical platform for colorimetric analysis of microfluidic device, Sens. Actuators, B 239 (2017) 52–59, https://doi.org/10.1016/j.snb.2016.07.159.
[18] S. Jafari, J. Guercetti, A. Geballa-Koukoula, A.S. Tsagkaris, J.L.D. Nelis, M.-P. Marco, J.-P. Salvador, A. Gerssen, J. Hajslova, C. Elliott, K. Campbell, D. Migliorelli, L. Burr, S. Generelli, M.W.F. Nielen, S.J. Sturla, ASSURED point-of-need food safety screening: a critical assessment of portable food analyzers, Foods 10 (2021) 1399, https://doi.org/10.3390/foods10061399.
[19] H.Y. Lin, C.H. Huang, J. Park, D. Pathania, C.M. Castro, A. Fasano, R. Weissleder, H. Lee, Integrated magneto-chemical sensor for on-site food allergen detection, ACS Nano 11 (2017) 10062–10069, https://doi.org/10.1021/acsnano.7b04318.
[20] R.K. Mishra, L.J. Hubble, A. Martín, R. Kumar, A. Barfidokht, J. Kim, M. M. Musameh, I.L. Kyratzis, J. Wang, Wearable flexible and stretchable glove biosensor for on-site detection of organophosphorus chemical threats, ACS Sens. 2 (2017) 553–561, https://doi.org/10.1021/acssensors.7b00051.
[21] T. Sergeyeva, D. Yarynka, E. Piletska, R. Linnik, O. Zaporozhets, O. Brovko, S. Piletsky, A. El, Development of a smartphone-based biomimetic sensor for aflatoxin B1 detection using molecularly imprinted polymer membranes, Talanta 201 (2019) 204–210, https://doi.org/10.1016/j.talanta.2019.04.016.
[22] X. Tang, R. Su, H. Luo, Y. Zhao, L. Feng, J. Chen, Colorimetric detection of Aflatoxin B 1 by using smartphone-assisted microfluidic paper-based analytical devices, Food Control 132 (2022), 108497, https://doi.org/10.1016/j.foodcont.2021.108497.
[23] Youxiu Lin, Q. zhou, Yuping Lin, Dianyong Tang, G. Chen, Dianping Tang, Simple and sensitive detection of aflatoxin B1 within five minute using a non-conventional competitive immunosensing mode, Biosens. Bioelectron. 74 (2015) 680–686, https://doi.org/10.1016/j.bios.2015.07.029.
[24] Z. Ben Abdallah, C. Grauby-Heywang, L. Beven, S. Cassagnere, F. Moroté, E. Maillard, H. Sghaier, T. Cohen Bouhacina, Development of an ultrasensitive label-free immunosensor for fungal aflatoxin B1 detection, Biochem. Eng. J. 150 (2019), https://doi.org/10.1016/j.bej.2019.107262.
[25] H. Bhardwaj, M.K. Pandey, G. Rajesh Sumana, Electrochemical Aflatoxin B1 immunosensor based on the use of graphene quantum dots and gold nanoparticles, Microchim. Acta 186 (2019), https://doi.org/10.1007/s00604-019-3701-5.
[26] F. Arduini, S. Cinti, V. Mazzaracchio, V. Scognamiglio, A. Amine, D. Moscone, Carbon black as an outstanding and affordable nanomaterial for electrochemical (bio)sensor design, Biosens. Bioelectron. 156 (2020), 112033, https://doi.org/10.1016/j.bios.2020.112033.
[27] G. Ibáñez-Redín, T.A. Silva, F.C. Vicentini, O. Fatibello-Filho, Effect of carbon black functionalization on the analytical performance of a tyrosinase biosensor based on glassy carbon electrode modified with dihexadecylphosphate film, Enzym. Microb. Technol. 116 (2018) 41–47, https://doi.org/10.1016/j.enzmictec.2018.05.007.
[28] T.W.B. Lo, L. Aldous, R.G. Compton, The use of nano-carbon as an alternative to multi-walled carbon nanotubes in modified electrodes for adsorptive stripping voltammetry, Sens. Actuators, B 162 (2012) 361–368, https://doi.org/10.1016/j.snb.2011.12.104.
[29] H. Kaan Kaya, N. Haghmoradi, B. Yarar Kaplan, F. Kuralay, Platinum nanoparticles loaded carbon black: reduced graphene oxide hybrid platforms for label-free electrochemical DNA and oxidative DNA damage sensing, J. Electroanal. Chem. 910 (2022), https://doi.org/10.1016/j.jelechem.2022.116180.
[30] A. Koterwa, I. Kaczmarzyk, S. Mania, M. Cieslik, R. Tylingo, T. Ossowski, R. Bogdanowicz, P. Niedziałkowski, J. Ryl, The role of electrolysis and enzymatic hydrolysis treatment in the enhancement of the electrochemical properties of 3D-printed carbon black/poly(lactic acid) structures, Appl. Surf. Sci. 574 (2022), https://doi.org/10.1016/j.apsusc.2021.151587.
[31] Y. Liu, H. Li, S. Gong, Y. Chen, R. Xie, Q. Wu, J. Tao, F. Meng, P. Zhao, A novel non-enzymatic electrochemical biosensor based on the nanohybrid of bimetallic PdCu nanoparticles/carbon black for highly sensitive detection of H2O2 released from living cells, Sens. Actuators, B 290 (2019) 249–257, https://doi.org/10.1016/j.snb.2019.03.129.
[32] P.B. Deroco, O. Fatibello-Filho, F. Arduini, D. Moscone, Effect of different carbon blacks on the simultaneous electroanalysis of drugs as water contaminants based on screen-printed sensors, Electroanalysis 31 (2019) 2145–2154, https://doi.org/10.1002/elan.201900042.
[33] S. Fatma, B.B. Prasad, S. Jaiswal, R. Singh, K. Singh, Electrochemical simultaneous analysis of dopamine and epinephrine using double imprinted One MoNomer acryloylated graphene oxide-carbon black composite polymer, Biosens. Bioelectron. 135 (2019) 36–44, https://doi.org/10.1016/j.bios.2019.04.016.
[34] A.P.P. Eisele, C.F. Valezi, T. Mazziero, R.F.H. Dekker, A.M. Barbosa-Dekker, E. R. Sartori, Layering of a film of carboxymethyl-botryosphaeran onto carbon black as a novel sensitive electrochemical platform on glassy carbon electrodes for the improvement in the simultaneous determination of phenolic compounds, Sens. Actuators, B 287 (2019) 18–26, https://doi.org/10.1016/j.snb.2019.02.004.
[35] D. Rojas, F. Della Pelle, M. Del Carlo, E. Fratini, A. Escarpa, D. Compagnone, Nanohybrid carbon black-molybdenum disulfide transducers for preconcentration-free voltammetric detection of the olive oil o-diphenols hydroxytyrosol and oleuropein, Microchim. Acta 186 (2019), https://doi.org/10.1007/s00604-019-3418-5.
[36] F. Arduini, S. Cinti, V. Caratelli, L. Amendola, G. Palleschi, D. Moscone, Origami multiple paper-based electrochemical biosensors for pesticide detection, Biosens. Bioelectron. 126 (2019) 346–354, https://doi.org/10.1016/j.bios.2018.10.014.
[37] European Commission, Commission Regulation (EU) No 519/2014 of 16 May 2014 amending Regulation (EC) No 401/2006 as regards methods of sampling of large lots, spices and food supplements, performance criteria for T-2, HT-2 toxin and citrinin and screening methods of analysis T, Off. J. Eur. Union L 147 (2014) 29–43, https://doi.org/10.1007/BF02321443.
[38] M. Oplatowska-Stachowiak, N. Sajic, Y. Xu, S.A. Haughey, M.H. Mooney, Y. Y. Gong, R. Verheijen, C.T. Elliott, Fast and sensitive aflatoxin B1 and total aflatoxins ELISAs for analysis of peanuts, maize and feed ingredients, Food Control 63 (2016) 239–245, https://doi.org/10.1016/j.foodcont.2015.11.041.
[39] F.-Y. Yu, A.v. Gribas, M.M. Vdovenko, I.Yu Sakharov, Development of ultrasensitive direct chemiluminescent enzyme immunoassay for determination of aflatoxin B1 in food products, Talanta 107 (2013) 25–29, https://doi.org/10.1016/j.talanta.2012.12.047.
[40] J.L.D. Nelis, D. Migliorelli, S. Jafari, S. Generelli, J. Lou-Franco, J.P. Salvador, M. P. Marco, C. Cao, C.T. Elliott, K. Campbell, The benefits of carbon black, gold and magnetic nanomaterials for point-of-harvest electrochemical quantification of domoic acid, Microchim. Acta 187 (2020) 1–11, https://doi.org/10.1007/s00604-020-4150-x.
[41] J.L.D. Nelis, D. Migliorelli, L. Mühlebach, S. Generelli, L. Stewart, C.T. Elliott, K. Campbell, Highly sensitive electrochemical detection of the marine toxins okadaic acid and domoic acid with carbon black modified screen printed electrodes, Talanta 228 (2021), 122215, https://doi.org/10.1016/j.talanta.2021.122215.
[42] J.L.D. Nelis, D. Migliorelli, S. Jafari, S. Generelli, J. Lou-Franco, J.P. Salvador, M. P. Marco, C. Cao, C.T. Elliott, K. Campbell, The benefits of carbon black, gold and magnetic nanomaterials for point-of-harvest electrochemical quantification of domoic acid, Microchim. Acta 187 (2020) 164, https://doi.org/10.1007/s00604-020-4150-x.
[43] F. Conzuelo, M. Gamella, S. Campuzano, A.J. Reviejo, J.M. Pingarrón, Disposable amperometric magneto-immunosensor for direct detection of tetracyclines antibiotics residues in milk, Anal. Chim. Acta 737 (2012) 29–36, https://doi.org/10.1016/j.aca.2012.05.051.
[44] A. Valverde, E. Povedano, V. Ruiz-Valdepeñas Montiel, P. Yáñez-Sedeño, M. Garranzo-Asensio, N. Rodríguez, G. Domínguez, R. Barderas, S. Campuzano, J. M. Pingarrón, Determination of cadherin-17 in tumor tissues of different metastatic grade using a single incubation-step amperometric immunosensor, Anal. Chem. 90 (2018) 11161–11167, https://doi.org/10.1021/acs.analchem.8b03506.
[45] A.J. Bard, Electrochemical Methods Fundamentals and Applications, second ed., J. Wiley, Hoboken, 2001.

[46] F. Arduini, S. Cinti, V. Mazzaracchio, V. Scognamiglio, A. Amine, D. Moscone, Carbon black as an outstanding and affordable nanomaterial for electrochemical (bio)sensor design, Biosens. Bioelectron. 156 (2020), 112033, https://doi.org/10.1016/j.bios.2020.112033.
[47] D. Wu, J. Voldman, An integrated model for bead-based immunoassays, Biosens. Bioelectron. 154 (2020), 112070, https://doi.org/10.1016/j.bios.2020.112070.
[48] J. Crowther, The ELISA guidebook, Methods Mol. Biol. (2009).
[49] Y. Fan, J. Liu, Y. Wang, J. Luo, H. Xu, S. Xu, X. Cai, A wireless point-of-care testing system for the detection of neuron-specific enolase with microfluidic paper-based analytical devices, Biosens. Bioelectron. 95 (2017) 60–66, https://doi.org/10.1016/j.bios.2017.04.003.
[50] P.B. Lillehoj, M.C. Huang, N. Truong, C.M. Ho, Rapid electrochemical detection on a mobile phone, Lab Chip 13 (2013) 2950–2955, https://doi.org/10.1039/c3lc50306b.
[51] A.C. Sun, D.A. Hall, Point-of-Care smartphone-based electrochemical biosensing, Electroanalysis 31 (2019) 2–16, https://doi.org/10.1002/elan.201800474.